1624–1634 *Nucleic Acids Research, 2018, Vol. 46, No. 4* *Published online 25 January 2018*
doi: 10.1093/nar/gky035

i-Motif of cytosine-rich human telomere DNA fragments containing natural base lesions

Zuzana Dvořáková[1], Daniel Renčiuk[1], Iva Kejnovská[1], Petra Školáková[1], Klára Bednářová[1], Janos Sagi[2] and Michaela Vorlíčková[1,*]

[1]Institute of Biophysics of the Czech Academy of Sciences, Královopolská 135, 612 65 Brno, Czech Republic and [2]Rimstone Laboratory, RLI, Carlsbad, CA 92010, USA

Received November 07, 2017; Revised January 08, 2018; Editorial Decision January 14, 2018; Accepted January 15, 2018

ABSTRACT

i-Motif (iM) is a four stranded DNA structure formed by cytosine-rich sequences, which are often present in functionally important parts of the genome such as promoters of genes and telomeres. Using electronic circular dichroism and UV absorption spectroscopies and electrophoretic methods, we examined the effect of four naturally occurring DNA base lesions on the folding and stability of the iM formed by the human telomere DNA sequence $(C_3TAA)_3C_3T$. The results demonstrate that the TAA loop lesions, the apurinic site and 8-oxoadenine substituting for adenine, and the 5-hydroxymethyluracil substituting for thymine only marginally disturb the formation of iM. The presence of uracil, which is formed by enzymatic or spontaneous deamination of cytosine, shifts iM formation towards substantially more acidic pH values and simultaneously distinctly reduces iM stability. This effect depends on the position of the damage sites in the sequence. The results have enabled us to formulate additional rules for iM formation.

INTRODUCTION

Endogenous biochemical reactions and exogenous effects can trigger the formation of reactive oxygen species (ROS) in cells, which react with various molecules in cells including biomacromolecules. Of these, nucleic acids are among the main macromolecular targets of ROS induced damage (1). The physical and biochemical effects of this damage has been thoroughly studied with double helical (2) and a few non-B DNA models, including the four-stranded G-quadruplexes (3–5). Another four-stranded non-canonical nucleic acid architecture is the i-motif (iM), which can also be targeted by intracellular ROS reactions.

Oligo- and polynucleotides with repeating cytosine (C)-rich sequences tend to form iM structures in slightly acidic conditions (6). The iM consists of two parallel stranded duplexes that are held together by hemi-protonated cytosine base pairs ($C{\cdot}C^+$) (Figure 1A) and are mutually intercalated in antiparallel orientation (Figure 1B). C-rich sequences of the human genome also form iM structures facilitated by negative superhelicity and crowding under physiological conditions. This implicates a biological role of this architecture (7–15). Due to the pH-dependence of iM formation, nanotechnology has been using iM-forming sequences as pH-switches, DNA-nanomotors and other DNA nano-devices (16,17). Earlier (7) as well as recent reviews (8,16,18) have evaluated many aspects of the sequence requirements, kinetics, topology and stability of iMs, their significance in gene expression, and in iM–ligand complex formation. Structural features of iMs have also been studied with nucleotide analogues, similarly to the other four-stranded non-B fold, the G-quadruplexes (4). However, the spectrum of the natural and synthetic building blocks used in iM studies is less comprehensive than with the G-quadruplexes. Primarily, 5-methylcytosine (5mC), an epigenetic modification has been studied in detail (13,19–24). Publications on ROS-induced damage include derivatives of 5mC: 5-hydroxymethylcytosine (5hmC), 5-formylcytosine and 5-carboxycytosine. These oxidized derivatives are not only intermediates of enzymatic demethylation of mC but also serve as epigenetic marks in mammals (13,20). The 5mC, except in the case of hypermethylation, stabilized (20), whereas 5hmC destabilized the iM (13). iMs fold near pH 6, but replacing C with 5mC shifts this pH towards neutral values, while replacing C with 5-bromocytosine (5BrC) shifts the pH to more acidic values (25). Regarding loop modifications, loop length and sequence have been found to significantly impact the thermodynamics and kinetics of the folding of iM DNA (26–31). The effect of substitutions of loop nucleotides of iMs has barely been studied (24,32–34).

We have long been interested in investigating the effect of natural base lesions on the folding topology of G-quadruplexes of the human telomere DNA sequence. We substituted G bases of the G-tetrads by derivatives of G, such as 8-oxoguanine (35) and an abasic site (36), and recently, by incorporating 8-oxoadenine (8oxoA), adenine

*To whom correspondence should be addressed. Tel: +420 541 517 188; Email: mifi@ibp.cz

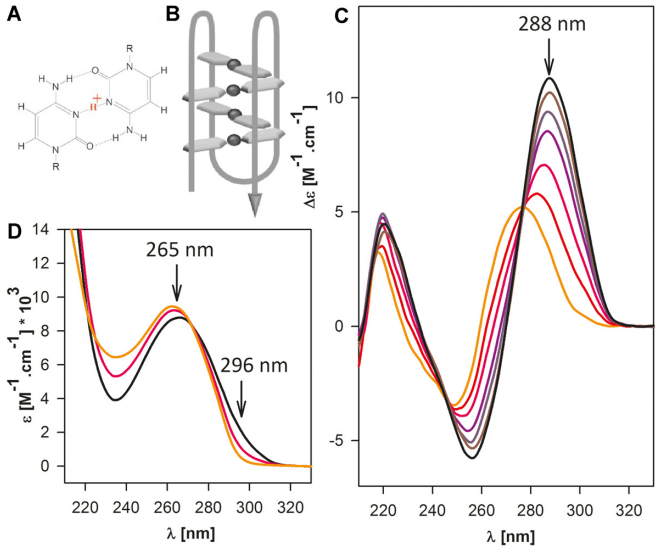

Figure 1. (**A**) A hemiprotonized C·C$^+$ base pair; (**B**) a schematic structure of an intramolecular iM; (**C**) CD and (**D**) UV absorption spectra reflecting iM formation induced by decreasing pH from 7.5 (orange) to 5.0 (black). The course of iM formation and unfolding is monitored by changes in Δε at 288 nm and ε at 296 nm, respectively, as indicated in the figure.

abasic sites and 5-hydroxymethyluracil into the TTA loops of the human telomere G-strand quadruplex (3). However, the effects of natural lesions in the complementary C-rich human telomere (htel) sequence have not been studied yet. Here, we present the results of the effects of the most frequently occurring natural base lesions within the loops and the core cytosines of the iM formed by the htel C-strand 22mer sequence, 5′-(CCCTAA)$_3$CCCT-3′. The study includes the influence of the 8oxoA, and the abasic site replacing 2′-deoxyadenosines, and 5hmU (37) substituting for thymine of the TAA loops, and of the uracil, the deamination product of core cytosines (38,39), on the formation and stability of the htel iM.

MATERIALS AND METHODS

Oligonucleotides

Loop-modified DNA sequences (Supplementary Table S1) were synthesized by the Department of Functional Genomics and Proteomics, Masaryk University, Brno (36), and the sequences with substitutions of U for C by Sigma-Aldrich (Haverhill, UK). The lyophilized samples were dissolved in 1 mM sodium phosphate (pH 8.0) with 0.3 mM EDTA. The purity of the samples in terms of length homogeneity was checked by denaturing gel electrophoresis. Before measurements, the DNA samples were thermally denatured in 1 mM sodium phosphate at 90°C for 5 min. Precise concentration of the studied sequences was determined based on UV absorption measured at 260 nm at 90°C using molar absorption coefficient of 8900 $M^{-1}\cdot cm^{-1}$ calculated for the wild type sequence of $(C_3TAA)_3C_3T$ according to Gray (40). The same coefficient was used for the loop-modified sequences. The extinction coefficients of 9000 and 9050 $M^{-1}\cdot cm^{-1}$ were used for one and two U/C core substitutions, respectively. UV absorption was measured on a UNICAM 5625 UV/VIS spectrometer (Cambridge, UK).

Circular dichroism

Circular dichroism spectra were measured on a Chirascan-plus CD spectrometer (Applied Photophysics, UK) in the region of 210–330 nm with 0.5 nm step and 0.5 s time-per-point. CD was expressed as a difference in molar absorption of left- and right-handed circularly polarized light (Δε) related to base. The measurement was performed at 23°C in 1 cm path-length quartz Hellma cells placed in a thermostated holder.

UV melting

Denaturation/renaturation curves were measured on a Varian Cary 4000 spectrophotometer in a K-RB buffer, pH 5 (specified below). The spectra were collected from 210 to 330 nm in the temperature range 1–85°C in four cycles (up, down, up and down) with 1°C step and 2 min of waiting at each temperature. The final temperature change rate was around 0.25°C·min^{-1}. Melting curves were monitored by absorbance at 296 nm, T_m values were determined from 0 to 1 normalized dependences (the bottom and upper linear baseline-corrected melting curves) as the temperature where half of the sample was folded (41). The error range of T_m determination was ±0.5°C.

pH measurements

pH dependences were measured on pH meter Mettler Toledo (with an In Lab Micro electrode) in Robinson-Britton (K-RB) buffer, which is a mixture of 0.04 M H_3BO_3, 0.04 M CH_3COOH and 0.04 M H_3PO_4 titrated with 0.2 M KOH to desired pH. The K^+ concentration was 0.07 M for pH 7. The oligonucleotides were titrated directly in cells by 0.2 M HCl and pH dependent changes were monitored by a set of values of Δε at 288 nm assembled from twenty spectra on average. The pK_a values were determined based on the 4-parameter Hill equation used to automatically fit the experimental points by a SigmaPlot software (Systat Software, USA). The error range of pK_a determination was ±0.05.

Native PAGE

The molecularity of oligonucleotides was determined from native polyacrylamide gel electrophoresis (PAGE) using an electrophoretic instrument (SE-600; Hoefer Scientific, San Francisco, CA, USA). Gel concentration was 16% and both the gel and the running buffer contained K-RB buffer, pH 5. About 2 μg of DNA was loaded on the gel. Electrophoresis ran at 30 V and 23°C for 18 h for samples with damaged loops and at 50 V and 4°C for 19 h for samples with damaged cytosines. Gels were stained with Stains All dye (Sigma-Aldrich, St. Louis, MO, USA) and scanned using a Personal Densitometer SI, model 375-A (Molecular Dynamics, Sunnyvale, CA, USA).

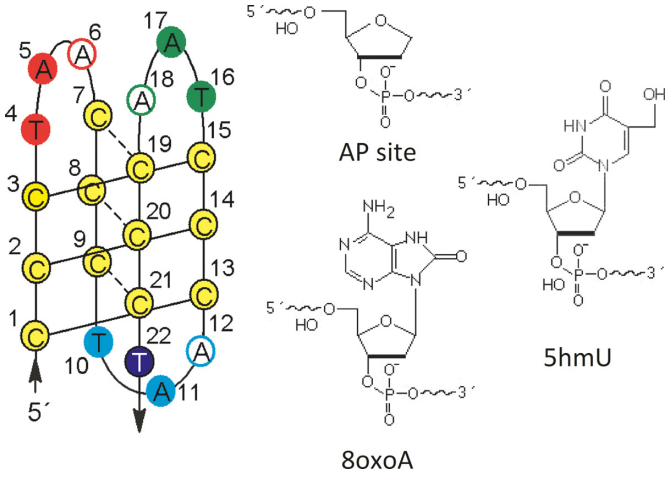

Figure 2. Schematic presentation of the htel iM with numbering and colors used for particular nucleotides referenced in the text and the figures in this paper; chemical structures of studied lesions.

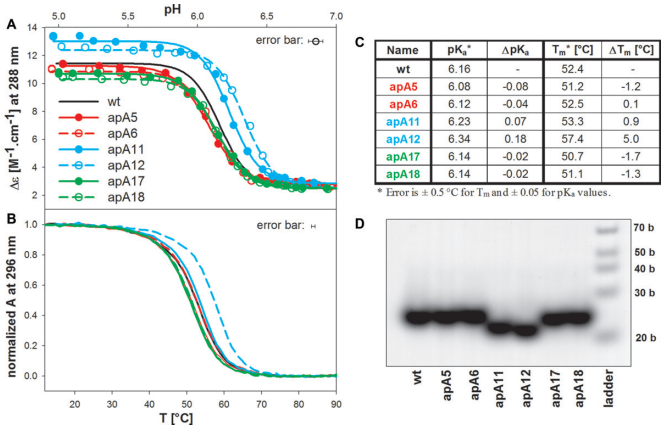

Name	pK_a*	ΔpK_a	T_m* [°C]	ΔT_m [°C]
wt	6.16	-	52.4	-
apA5	6.08	-0.08	51.2	-1.2
apA6	6.12	-0.04	52.5	0.1
apA11	6.23	0.07	53.3	0.9
apA12	6.34	0.18	57.4	5.0
apA17	6.14	-0.02	50.7	-1.7
apA18	6.14	-0.02	51.1	-1.3

* Error is ± 0.5 °C for T_m and ± 0.05 for pK_a values.

Figure 3. (**A**) pH dependent iM formation of the AP/A site containing htel sequences monitored by Δε at 288 nm; (**B**) normalized melting curves monitored by UV absorption at 296 nm, (**C**) table of pK_a and T_m values, (**D**) the 16% native PAGE. The measurements were carried out in K-RB, pH 5 for melting and electrophoresis, and at 23°C for the pH dependence and electrophoresis as stated in the M+M section.

RESULTS

Formation of an i-motif (iM) is sensitively reflected in the spectra of the electronic circular dichroism (Figure 1C) and in UV absorption spectra (Figure 1D). A single-stranded unordered C-rich human telomere (htel) DNA fragment yields a CD spectrum with a positive maximum at 275 nm and a negative one around 245 nm. With decreasing pH below pH 7, the sequence forms an iM, which is reflected by an increase of the positive CD band and a simultaneous decrease of the negative one, while the whole spectrum shifts towards the red. CD spectrum with a positive maximum at 288 nm and a negative one close to 260 nm is characteristic of the iM (Figure 1C). Cytosine protonation is reflected by an increase in the UV absorption spectrum around 300 nm and the formation of the ordered iM is accompanied by a decrease of the 265 nm maximum and a slight bathochromic shift (Figure 1D) (11,42).

Lesions in iM loops

We examined three types of damage which frequently occur in T and A bases forming TAA loops in the human telomere C-rich DNA sequence $(C_3TAA)_3C_3T$. Adenines were replaced by the abasic (AP) sites or 8-oxoadenines (8oxoA), and thymines were replaced by 5-hydroxymethyluracils (5hmU). The studied sequences are called apAX, 8oxoAX or 5hmUX, where X corresponds to the order of the substituted nucleobase in the studied htel 22-mer. All the studied sequences are listed in Supplementary Table S1. A scheme of the iM structure with the numbering of particular nucleobases is shown in Figure 2.

Adenine abasic (AP/A) sites. Figure 3A shows a pH-induced formation of iM by htel sequences containing AP lesions instead of particular loop A (AP/A). The iM formation is monitored by changes in CD values of its characteristic positive band (Figure 1C). The presence of AP/A lesions in the first and the third loops has virtually no effect on the formation of iM: Δε at 288 nm as a function of pH follows very closely the curve of the htel wild type (wt) sequence. The transition takes place in the region of pH 6.5–5.8 (Figure 3A), with the midpoint of pH ~6.12 (Figure 3C). Only the AP/A sites in the middle loop affect iM formation significantly. The transition midpoint of apA12 is shifted by 0.18 towards neutral pH. Changes in pK_a of other sequences are below the accuracy of their determination. The resulting iMs of apA11 and apA12 reach higher Δε values than the iM of the wt (Figure 3A). The AP sites in the middle loop increase the thermostability of the htel iM structure by 0.9 and 5°C for apA11 and apA12, respectively compared with the wt. In contrast, AP sites in the third, 3′end loop, slightly destabilize the iM (Figure 3B and C). The temperature dependences are fully reversible.

The presence of the AP sites does not alter the molecularity of the iM. All the structures are intramolecular. The missing bases in the middle loop slightly accelerate the migration of the structure (Figure 3D), probably indicating increased compactness of the structures.

8-oxoadenine (8oxoA) substitution for adenine. pH induced iM formation of 8oxoA htel analogues is shown in Figure 4A. With the exception of 8oxoA11, the presence of the oxo group stabilizes iM formation (Figure 4B and C) and shifts its formation towards neutral pH values for 8oxoA12 and the sequences substituted in the third loop. The effect of 8oxoA substitution in the middle loop is distinct for 8oxoA11 and 8oxoA12. 8oxoA12 forms the most stable and 8oxoA11 the least stable iM. The midpoint of the 8oxoA11 transition to iM is comparable with that of the wt, but it proceeds with lower cooperativity and the CD spectrum of the final iM reaches a lower Δε value (Figure 4A). The temperature dependences of all sequences are fully reversible. The 8oxoA/A substitution does not change the molecularity and all iMs remain intramolecular (Figure 4D).

5-hydroxymethyluracil (5hmU) substitution for thymine. The presence of the 5hmU influences only slightly iM for-

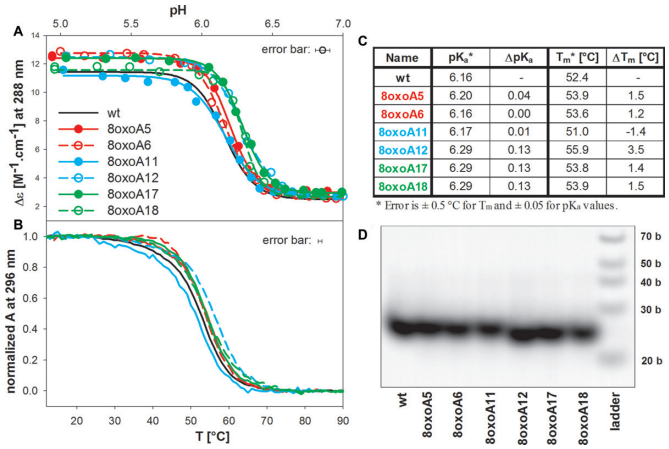

Name	pK_a*	ΔpK_a	T_m* [°C]	ΔT_m [°C]
wt	6.16	-	52.4	-
8oxoA5	6.20	0.04	53.9	1.5
8oxoA6	6.16	0.00	53.6	1.2
8oxoA11	6.17	0.01	51.0	-1.4
8oxoA12	6.29	0.13	55.9	3.5
8oxoA17	6.29	0.13	53.8	1.4
8oxoA18	6.29	0.13	53.9	1.5

* Error is ± 0.5 °C for T_m and ± 0.05 for pK_a values.

Figure 4. (**A**) pH dependent iM formation of the 8oxoA containing htel sequences monitored by Δε at 288 nm; (**B**) normalized melting curves monitored by UV absorption at 296 nm, (**C**) table of pK_a and T_m values, (**D**) the 16% native PAGE. The conditions are as in Figure 3.

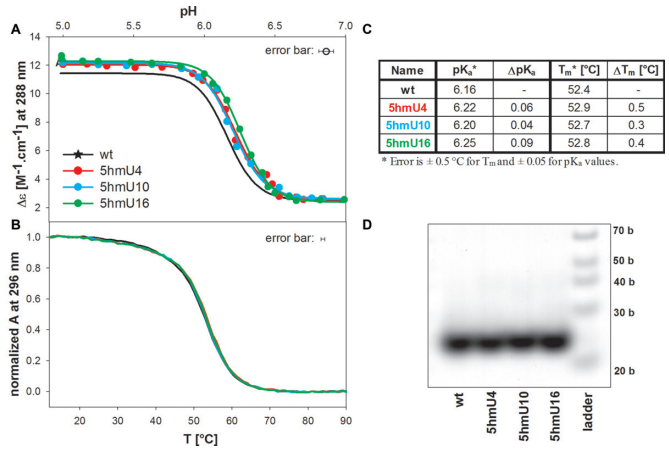

Name	pK_a*	ΔpK_a	T_m* [°C]	ΔT_m [°C]
wt	6.16	-	52.4	-
5hmU4	6.22	0.06	52.9	0.5
5hmU10	6.20	0.04	52.7	0.3
5hmU16	6.25	0.09	52.8	0.4

* Error is ± 0.5 °C for T_m and ± 0.05 for pK_a values.

Figure 5. (**A**) pH dependent iM formation of the 5hmU containing htel sequences monitored by Δε at 288 nm; (**B**) normalized melting curves monitored by UV absorption at 296 nm, (**C**) table of pK_a and T_m values, (**D**) the 16% native PAGE. The conditions are as in Figure 3.

mation (Figure 5) and the changes in T_m and pK_a are within or close to the accuracy of their determination. Final iMs of the substituted sequences yield slightly higher Δε values than the wt (Figure 5A). The modification influences neither the molecularity of the iMs nor affects distinctly their thermostability (Figure 5B, C and D).

Substitution of core cytosines by uracil

The htel sequences with particular deoxycytosines (Cs) substituted by deoxyuracil (U) are called UX in analogy with the loop-modified sequences (X corresponds to the order of the nucleobase in the $(C_3TAA)_3C_3T$ DNA sequence). Their primary structures are given in Supplementary Table S1. The pH-induced formation of iMs of the sequences monitored by Δε at 288 nm is shown in Figure 6A. The modifications have negative influence on iM formation. The transition shifts to more acidic values and simultaneously samples are thermally destabilized compared to the non-modified wt sequence (Figure 6B and C).

In the CCC trimer, the substitution of the external cytosines (with odd number positions) by U (U/C) maintains intramolecular folding of the iM but shifts its formation by 0.36 pH units on average to more acidic pH (Figure 6A and B). Their final iM structures reach lower values of Δε than the wt. U1 displays the highest Δε of all modified sequences, which indicates that its iM is least affected by the loss of the 5′ end C (C1) and it is (together with its counterpart U13) the most stable of the modified sequences. In contrast, U21 with a substituted 3′end C (C21), is the least stable structure (Figure 6B and C). U1 transforms into iM at a lower pK_a value than the odd number U3 in the same block. This first C block is, however, an exception. In all other blocks, the sequences with higher position numbers (U9, U15 and U21) display higher Δε than the preceding odd number sequences (U7, U13 and U19) (Figure 6A). Destabilization of the iM by the loss of cytosine-forming pair is similar for U1 and U13 (43.1°C, 42.9°C), and for U3 and U15 (41.7°C, 41.9°C), and becomes different towards the molecule end, i.e. T_m of U7 and U19 (39.9°C and 41.4°C, respectively), and of U9 and U21 (40.2°C and 37.7°C, respectively). The kinetics of iM formation of all odd sequences is rapid and their melting and renaturation proceed along the same curve (an example is shown in Supplementary Figure S1A).

The substitution of the inner (middle) cytosines in the CCC blocks (in even positions) is accompanied by much more extensive iM destabilization than the substitution of odd positions. Mainly, the U/C substitution in the even positions hinders intramolecular folding of the sequence so that all four inner U/C sequences form bimolecular iMs (Figure 6D). The electrophoresis shown in Figure 6D ran at low temperature. On the electrophoresis running at room temperature, all the odd-number sequences remain intramolecular but the even-number sequences provide, in addition to bimolecular species, a slight band in the middle between intramolecular and bimolecular species corresponding to low content of unstructured forms (Supplementary Figure S2). The bimolecular iMs display lower Δε values than the odd-number sequences (Figure 6A), their formation proceeds at much lower pH values, and the kinetics of the process are slow. The slow kinetics results in a distinct hysteresis between melting and iM reformation (Supplementary Figure S1B). Moreover, the denaturation profile corresponding to intermolecular iMs could not be fitted by a single sigmoidal curve (denaturation probably consists of multiple steps) so that the temperature of the midpoint of the renaturation curves (T_{ren}) was used for the comparison of iM thermostabilities of all the U/C substituted sequences (T_{ren} is identical with T_m for intramolecular motifs). The ΔT_{ren} of the bimolecular iMs is about 30°C lower and pK_a is shifted on average by nearly 0.7 pH units toward acid pH compared to the iM of the wt.

Clustered U/C substitutions. In the following study, we combined U/C substitutions in various htel sequence positions. The pK_a and T_{ren} values of the sequences are given in Figure 7A. Changes in pK_a and T_{ren} values well correlate in the whole set of U/C substituted sequences (Supple-

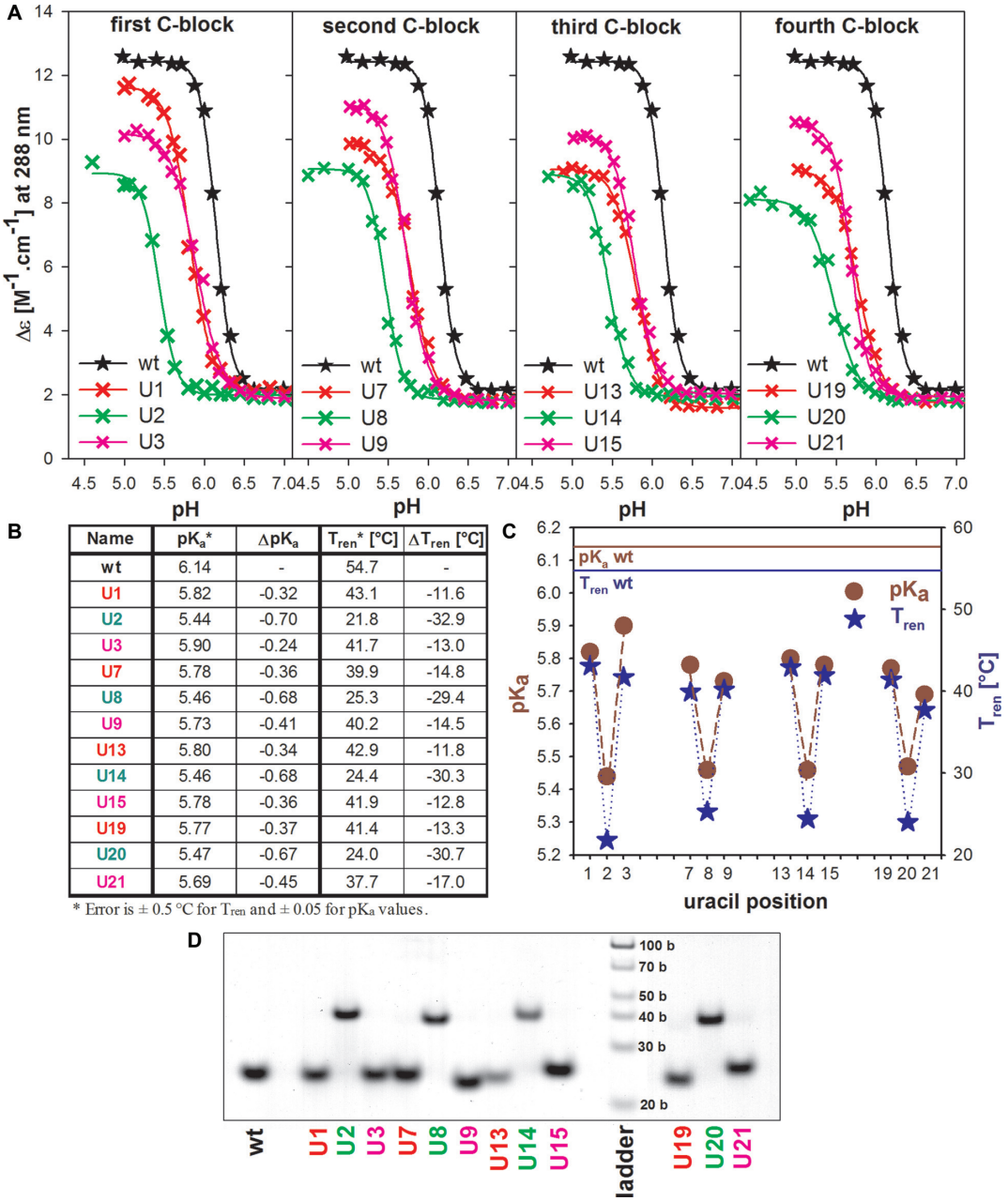

Name	pK_a*	ΔpK_a	T_{ren}* [°C]	ΔT_{ren} [°C]
wt	6.14	-	54.7	-
U1	5.82	-0.32	43.1	-11.6
U2	5.44	-0.70	21.8	-32.9
U3	5.90	-0.24	41.7	-13.0
U7	5.78	-0.36	39.9	-14.8
U8	5.46	-0.68	25.3	-29.4
U9	5.73	-0.41	40.2	-14.5
U13	5.80	-0.34	42.9	-11.8
U14	5.46	-0.68	24.4	-30.3
U15	5.78	-0.36	41.9	-12.8
U19	5.77	-0.37	41.4	-13.3
U20	5.47	-0.67	24.0	-30.7
U21	5.69	-0.45	37.7	-17.0

* Error is ± 0.5 °C for T_{ren} and ± 0.05 for pK_a values.

Figure 6. (**A**) pH dependent iM formation of the uracil containing htel sequences monitored by Δε at 288 nm, (**B**) Table of pK_a and T_{ren} (renaturation temperature) values, (**C**) dependence of pK_a (brown circles) and T_{ren} (blue stars) values on uracil position, (**D**) the 16% native PAGE. The measurements were carried out as shown in Figure 3 but the electrophoresis ran at 4°C.

mentary Figure S3). iMs were not properly formed for some U/C combinations so that T_{ren} could not be determined.

Sequences with two substituted Us for the outside (odd number) Cs localized in distinct C blocks (Figure 7, cyan, blue and violet) preferentially fold into intramolecular iMs. Those in opposite (parallel oriented) blocks form intramolecular iMs exclusively (Figure 7C, blue and violet). iM of U1,13 with a substituted first C·C$^+$ pair from the 5′end, is the least destabilized of all double U/C combinations - by 11.4°C (Figure 7A), which corresponds well with the destabilization of single substituted U1 or U13 (11.6 and 11.8°C). iMs of further sequences with two outside U/C substitutions replacing whole C·C$^+$ pair (Figure 7, blue), U7,19, U3,15 or U9,21 are destabilized by 14.1, 16.7 and 17.6°C, respectively (Figure 7A, right) and those with U/C substitutions replacing Cs of two different pairs (Figure 7, violet), U1,15 and U3,13 are destabilized by 13.1°C and 13.7°C, respectively.

U/C substitutions in neighbouring (antiparallel-oriented) C blocks (Figure 7, cyan), U1,7, U1,9 and U3,9, are destabilized by 26.0, 24.9 and 24.5°C compared to wt, i.e. significantly more than the previous sequences and more than the two respective single mutants. They predominantly fold intramolecularly but, in addition,

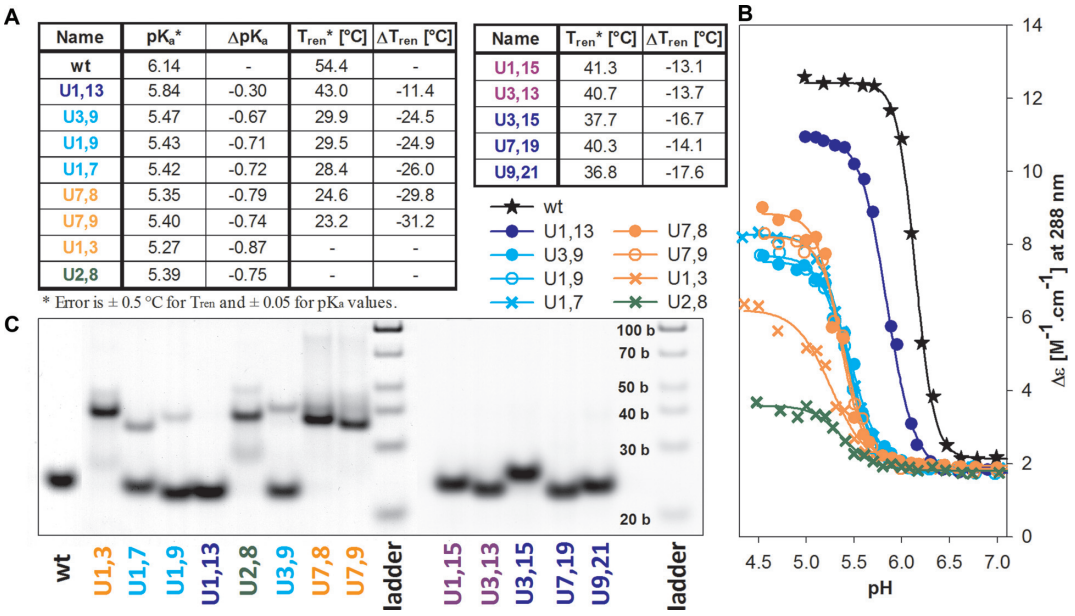

Name	pK_a*	ΔpK_a	T_{ren}* [°C]	ΔT_{ren} [°C]
wt	6.14	-	54.4	-
U1,13	5.84	-0.30	43.0	-11.4
U3,9	5.47	-0.67	29.9	-24.5
U1,9	5.43	-0.71	29.5	-24.9
U1,7	5.42	-0.72	28.4	-26.0
U7,8	5.35	-0.79	24.6	-29.8
U7,9	5.40	-0.74	23.2	-31.2
U1,3	5.27	-0.87	-	-
U2,8	5.39	-0.75	-	-

* Error is ± 0.5 °C for T_{ren} and ± 0.05 for pK_a values.

Name	T_{ren}* [°C]	ΔT_{ren} [°C]
U1,15	41.3	-13.1
U3,13	40.7	-13.7
U3,15	37.7	-16.7
U7,19	40.3	-14.1
U9,21	36.8	-17.6

Figure 7. (**A**) Table of pK_a and T_{ren} values of the two uracils containing htel sequences (colors differentiate particular types of mutual U positions); (**B**) pH dependent iM formation monitored by Δε at 288 nm and room temperature; (**C**) the 16% native PAGE at pH 5 and 4°C. Conditions as stated in M+M section.

they provide a band on the electrophoresis (Figure 7C) corresponding to a slight population of bimolecular iMs. The sequences are unstructured at room temperature as follows from the electrophoresis shown in Supplementary Figure S2.

Sequences containing both substitutions in the same block (U1,3, U7,8 and U7,9) (Figure 7, orange) are strongly destabilized: They form only intermolecular iMs and only partly at room temperature and at still lower pH values (Figure 7C and Supplementary Figure S2). U7,8 and U7,9 provide, in addition to bimolecular, very little populated four molecular structures at low temperature (Figure 7C).

iMs of sequences with substituted two inner (even number) cytosines by U are destabilized heavily so that T_{ren} of their formation cannot be determined. U2,8 (Figure 7, green) forms iM only partly at low temperatures and/or at very acidic pH around 4.5. A band corresponding to the presence of unstructured form is visible on the electrophoresis even at low temperature (Figure 7C). Similarly, U2,20 and U8,14 form iM only intermolecularly at low temperature (Supplementary Figure S4, green). U8,14 assembles into four-molecular iM in addition to bimolecular one. Interestingly, the substitution of two inner cytosines forming C·C^+ pair, as it is with U2,14 and U8,20, preserves, in addition to bimolecular, an intramolecular iM folding (Supplementary Figure S4, dark green). The intramolecular folding even prevails for U2,14.

Other sequences with still more U/C substitutions are listed in Supplementary Tables S1 and S2 and their electrophoresis at low temperature is shown in Supplementary Figure S4. At room temperature, these sequences provide one clear electrophoretic band corresponding to unstructured form (not shown). Substitutions of all three Cs in the blocks for U have a similar effect to two U/C substitutions in the same C-block. Bimolecular iM is observed for U1,2,3 and bimolecular and a smear of higher order forms for U7,8,9 at low temperature running electrophoresis (Supplementary Figure S4). U1,2,3,19,20,21 with two fully substituted C blocks, forms bimolecular iM, in addition to unstructured forms, and U7,8,9,13,14,15 forms a slightly faster running bimolecular iM (Supplementary Figure S4).

DISCUSSION

Numerous studies have been performed to uncover the effect of natural lesions of nucleotides on the structure and stability of G-quadruplexes (reviewed in 43). It has been demonstrated with G-quadruplexes of the G-rich htel DNA sequence that the impact of lesions depends on the type and location of the damage in the sequence: Lesions formed in the TTA loops either destabilize, do not affect or in some cases even stabilize the G-quadruplex (3,44–46), and can change the folding topology. For instance, abasic (AP) sites substituting for adenine nucleotides stabilize double-chain-reversal folding of the loops and induce the formation of hybrid quadruplexes (3,45). The presence of AP sites in all three loops transforms the quadruplex into parallel form (47). On the other hand, 8-oxoadenine slightly stabilizes the htel G-quadruplex without affecting its folding type (3,44). Depending on the folding topology, the majority of lesions formed in the core guanines destabilize the G-quadruplex (35,36,48) and, chiefly, restrict its conformational variability (47). Nevertheless, none of the single natural modifications present in G-rich sequences studied so far can hinder their folding into intramolecular G-quadruplexes. Only the clustering lesions prove to be deleterious for the folding or, depending on their position in the molecule, can ruin a G-quadruplex structure. No analogous studies with the same type of natural lesions as those found in htel G-quadruplex

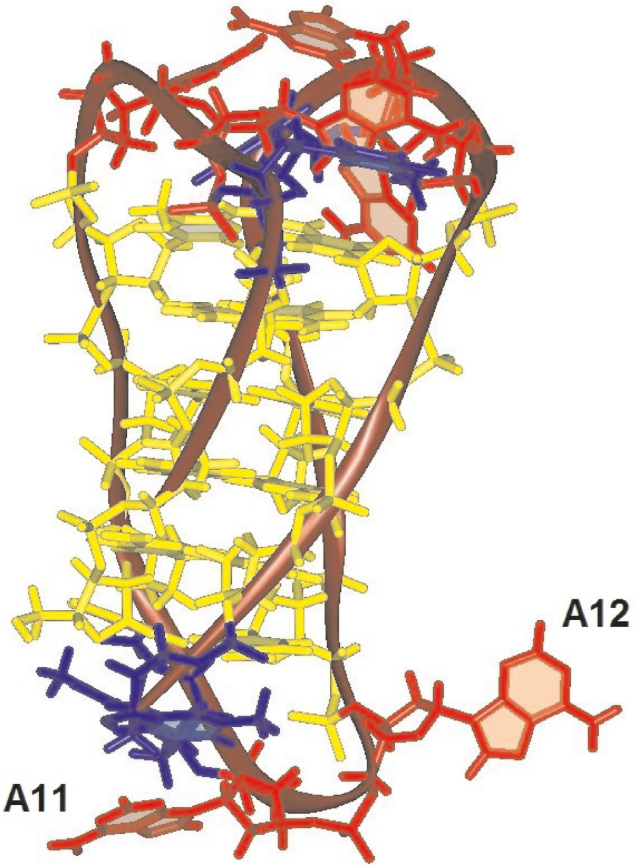

Figure 8. The 3D structure of human telomere sequence (PDB structure 1ELN). Cytosines are marked with yellow, adenines with red and thymines with blue color.

models have been conducted with iM structures forming from the C-rich htel sequences. Results presented in this paper are the first such evaluations. Similarly to the results for G-quadruplexes, the impact of lesions in iMs has been found here to be different in the TAA loops and in the core cytosines (Supplementary Table S1).

Loop damage

In contrast to G-quadruplexes, iMs cannot change their topology so that lesions in TAA loops of the C-rich htel sequence cause mostly minor changes in the formation and stability of its iM (overall data in Supplementary Table S1). This holds for all three modifications studied here, namely adenine abasic sites (apA), 8-oxoadenine (8oxoA) substituting adenines and 5-hydroxymethyluracil (5hmU) substituting thymines. None of these loop modifications, as in the case of htel G-quadruplexes, change the molecularity of the htel iMs.

Adenine is a large base, and the two purines probably cannot squeeze into the narrow space so that they protrude out of the iM core as shown in Figure 8. It can be expected that removing this flanking base will contribute to the stability of the iM structure as well as to its compactness. Missing A11 results in only slight iM stabilization and a shift of its formation toward less acidic pH. These changes are more extensive with A12. The released space upon the loss of one adenine may be filled by the other one so that the iM becomes more compact, which is observed on the PAG electrophoresis (Figure 3D). No important base interactions take place with adenines in the major grooves so that their loss does not significantly affect iM formation or stability.

In the case of the replacement of adenines by 8-oxoadenine, the iM formation is slightly stabilized and its formation is shifted to less acidic pH values. This is obvious with sequences substituted in the third loop, thus at the 3′ end. Similarly to the iMs, the stabilizing effect of the 8oxo group in loop adenines of htel G-quadruplexes was also observed (3,44) and it was argued (44) that it was the first example among the natural DNA lesions that stabilized the htel G-quadruplex DNA. Interestingly, the 8oxoA substitution has a different effect in the case of 8oxoA11, which forms the least stable iM of all modified samples, and for 8oxoA12, the iM of which is the most stable. Oxygen on the carbon C8 of the adenine A11 may cause a steric problem which may be responsible for the observed slight iM destabilization. In contrast, the oxygen on A12 may drag the base closer to the iM core, likely to T22, and prevent its fluctuation. With increasing stability of the iM, the structure becomes more compact and this can be traced on the PAGE electrophoresis of 8oxoA12 (Figure 4D).

Substitution of thymines by 5hmU does not, within the accuracy of the measurement, influence iM stability. The explanation may follow from the PDB structures of iM (1ELN and 1EL2) (49) according to which it seems that thymines do not participate in any stacking or binding interactions.

Substitution of core cytosines by uracil

A substitution of core cytosines by uracil devastates iM structure much more than the damage of loops (Supplementary Table S1), as a single U/C substitution causes the loss of one $C{\cdot}C^+$ pair and thus an extensive destabilization of the structure. A loss of outer (odd number) cytosines does not hinder intramolecular iM folding but the iMs are formed at lower pH values (ΔpK_a 0.24–0.45) and are by 11.6–17.0°C less stable than iM of the wt. It follows from Figure 6C that the readiness of iM formation slightly decreases with the location of the substituted C closer to 3′end. The most stable is the iM of U1 and its pairing counterpart U13, followed by U3 and the counterpart U15, and the least stable of the odd-number sequences is U21. U1 behaves atypically: It displays the highest $\Delta\varepsilon$ value of all modified structures so that its iM is least deformed by the substitution. Despite its least destabilization, it forms iM at slightly lower pH than U3. The opposite is true for all other odd number U/C substitutions: U7, U13 and U19 display lower $\Delta\varepsilon$ values than respective U9, U15, and U21. Their structures are thus more affected by the sequence modification, but their iMs are less destabilized. The order of stability of the odd-number substituted sequences is: U1>U3, U7∼U9, U13>U15 and U19>U21.

Intramolecular iMs can adopt two distinct intercalation topologies differing in the position of the intercalated pairs (50,51). The structure with the outermost $C{\cdot}C^+$ pair containing 5′C (C1) (Figure 9A, left) is called 5′E, and the structure, in which the outermost pair contains 3′end C (C21) is called 3′E structure (Figure 9A, right). The above men-

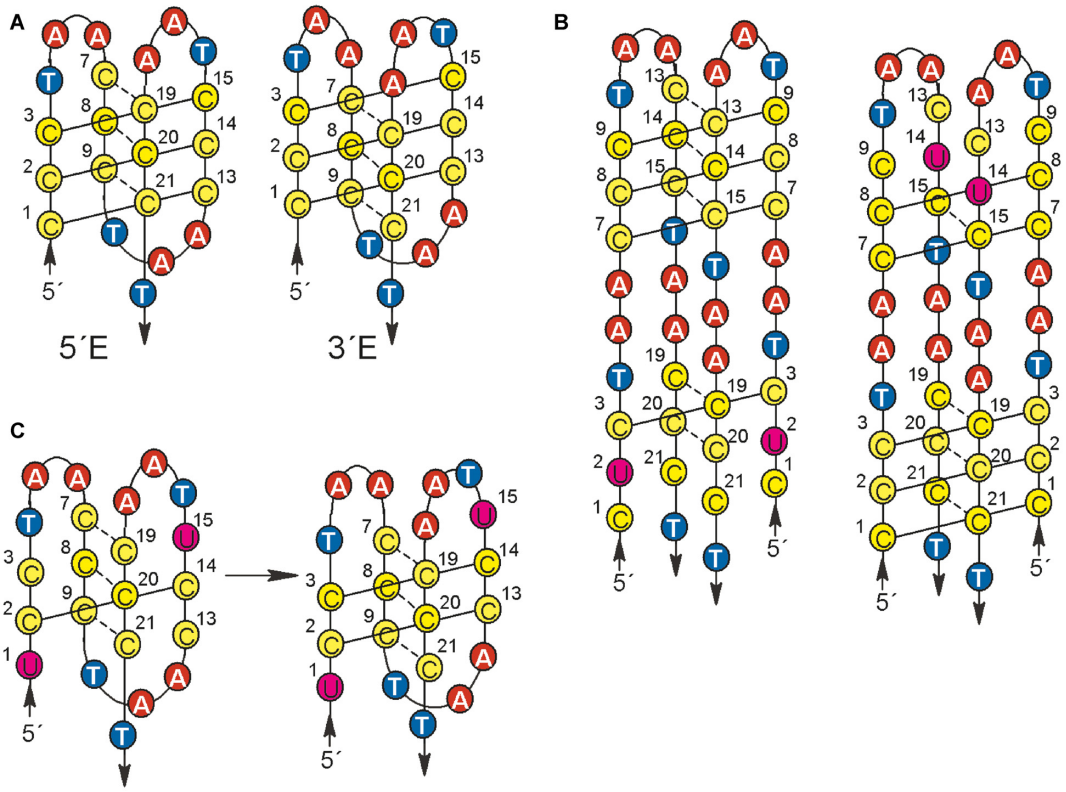

Figure 9. (**A**) Possible 5′E and 3′E topologies of intramolecular wt iM (49,51); (**B**) suggested structures of bimolecular iM of U2 and U14; (**C**) a shift in C·C$^+$ pairing of U1,15.

tioned order in iM destabilization by U/C substitution indicates that C3, C15 and C21 may be situated inside the iM. The substitution of inner pairs is more deleterious for iM stability as it results in the loss of one pair intercalated between two inversely oriented pairs, thus in the loss of the regular alternation of parallel and antiparallel C·C$^+$ pairs. This situation would come up if the iM adopted 5′E arrangement, which is drawn in the schematic presentation in Figure 2.

The substitution of the middle, thus even-numbered Cs by U causes much more distinct destabilization than in the case of the odd-number ones. Mainly, these sequences are no longer able to fold intramolecularly. The iM can only fold intermolecularly (Figure 6D). This is a distinction from the effect of modified guanines in the middle tetrad of htel G-quadruplexes where formation of some amount of bimolecular, sometimes also tetramolecular species have been observed (35,36,52) but the intramolecular quadruplexes always dominated. In this respect, the C-rich htel strand is more vulnerable than the G-rich strand as the damage of the middle C of the C triad within a long molecule makes the respective region incapable to form iM.

Bimolecular iMs consist of two units separated by TAA triplets (Figure 9B). The stability of the bimolecular iMs decreases in the order of U8, U14, U20, U2 (Figure 6C). Bimolecular iM is thus more stable if it contains the complete number of six C·C$^+$ pairs at the end of the structure than on the side of the loops (Figure 9B). Thus, the part close to the loop copes with the loss of the middle pair better than the end part. Based on the analogy with the intramolecular iMs, the part with the U in the middle of the sequence would be unable to form iM. It can be thus expected that the TAA loop forms a bulge and the remaining part with the rest of not damaged C·C$^+$ pairs can stack on the complete six pair iM.

Based on simultaneous substitutions of two Cs by Us, we can assess the following simple rules of iM folding. Depending on the mutual position of the substituted C, several variants may occur:

A. Substituted outer (odd number) cytosines
   a1) in parallel oriented chains and pairing cytosines: Substitutions of Cs involved in pairing lead to demotion of this C·C$^+$ pair from the motif, while its intramolecular folding is preserved. U1,13 forms the most stable iM. The same thermostability and pK_a of the iM formation of U1,13 (blue in Figure 7) as of the single substituted U1 and U13 indicates that with the loss of one of these pairing cytosines the whole pair is lost and, simultaneously, that C with U do not pair at acidic pH. Further examples of this type of damage are U3,15, U7,19 and U9,21 (Figure 7A, right). All lack one C·C$^+$ pair but still form intramolecular iMs (Figure 7C). It follows from the preceding results that the iM stability is more affected by the loss of inner than outer C·C$^+$ pairs that do not disturb alternating C·C$^+$ pairing of parallel and antiparallel oriented

chains. A comparison of the distinctly higher T_{ren} of U1,13 (43.0°C) than U3,15 (37.7°C) and, in the same way, higher T_{ren} of U7,19 (40.3°C) than of U9,21 (36.8°C) (Tables A in Figure 7) again supports that the htel iM adopts 5′E motif, in which the less vulnerable C1·C13$^+$ and C7·C19$^+$ pairs are situated outside the iM core (Figure 9A, left). Just the 5′E structure was found by NMR (51) as a major conformation in an equilibrium of htel-21 $(C_3TAA)_3C_3$ iM conformers.

a2) in parallel oriented chains and cytosines that do not pair: (Examples are U1,15 and U3,13 (violet in Figure 7A and C) with cytosines situated cornerwise.) Though this damage concerns two pairs, their iMs are relatively little destabilized (by 13.1°C and 13.7°C) and the structure remains predominantly intramolecular (Figure 7C). This indicates that a shift in C pairing takes place so that only one C·C$^+$ pair is lost (Figure 9C).

b) in antiparallel oriented chains: (Examples are U1,7, U1,9 or U3,9 (cyan in Figure 7). Destabilization of their iMs is more distinct than in the case of previous sequences, namely 26.0°C, 24.9°C and 24.5°C, respectively. Similar shift in C·C$^+$ pairing may occur in analogous cases (Supplementary Figure S5). Four C pairs remain preserved, which still allows the formation of an intramolecular structure, though a minority presence of bimolecular fraction can be traced on the electrophoresis (Figure 7C).

B. Substituted inner (even number) cytosines: These substitutions (Figure 7 and Supplementary Figure S4, green) destabilize iM distinctly, so that the sequences form iMs only partly at room temperature and T_{ren} values cannot be determined (Supplementary Table S2). They all form bimolecular iMs at low temperatures but distinctly populated depending on mutual positions of the inner U/C substitutions. Those in the first and third or second and fourth C blocks (light green in Supplementary Figure S4), parallel-oriented in the intramolecular arrangement, occur in the same parts of the bimolecular iMs: In the first case, they are in the part at the molecule ends, in the second case, in the part close to the loop. The latter sequence forms, in addition, tetramolecular iMs. U/C substitutions in neighbouring C blocks (first and second or third and fourth C blocks) occur in both parts of the bimolecular iM so that both its regions are affected. Population of unstructured forms can be found on their low temperature electrophoresis pattern (Figure 7C and Supplementary Figure S4). On the other hand, the substitutions of Cs, which form pairs in intramolecular iM, remain to a large extent intramolecular (Supplementary Table S2 and Supplementary Figure S4, dark green).

C. Substituted cytosines in the same block (orange in Figure 7 and Supplementary Figure S4): These substitutions also have a large devastating effect on iM formation. None of these sequences form intramolecular iMs. Bimolecular structures are formed at low temperature and a part of molecules remains still unstructured or four-molecular iMs are formed with some sequences (Figure 7C). The structures melt around room temperature. In all these sequences, one part of the bimolecular iMs contains only one and three C·C$^+$ pairs, probably stacked on the second intact iM part. The part with possible one and three C·C$^+$ pairs contributes only marginally to the bimolecular iM stability as the sequences with the whole U/C substituted block (U1,2,3 or U7,8,9) behave similarly on the electrophoresis (Figure 7C and Supplementary Figure S4). Also in this case, the two or three substitutions in the region close to the loop are better tolerated than those situated at the molecule ends. The sequences with U/C in the regions close to the loops are more susceptible to form four-molecular iMs (Supplementary Figure S4).

It can be concluded that for the formation of an intramolecular iM, the presence of two and three or at least two and two regularly alternating parallel and antiparallel C·C$^+$ pairs are required. On violation of the regular alternation of parallel and antiparallel oriented intercalated pairs (by a loss of the middle C), exclusively bimolecular iMs are formed. In the case of a bimolecular iM, two and one alternating parallel antiparallel pairs are tolerated as well, which then probably stack on the intact six C·C$^+$ pairs containing iM of the second part of the molecule. The damage in the region close to the iM loop is then better tolerated than at the end of the molecule.

The presented results show that the effect of naturally forming lesions on htel DNA differs depending on the position of the damage. The three different lesions studied occurring in loops did not substantially change intramolecular structure of htel iM, while the C-to-U lesion targeting iM core and especially their clusters, which may be formed by e.g. ionizing irradiation, are more deleterious for the iM structure and stability. Even a single C damage within a three C block is more dangerous than the analogous damage in the complementary G-rich htel sequence as it hinders intramolecular iM folding and thus makes iM formation impossible in the appropriate region of the C-rich DNA molecule. Recently, a considerable amount of experimental evidence has accumulated proving that not only G-quadruplexes but also iMs are important biological elements controlling DNA function, namely gene expression (53–57). In this respect, it is essential to note the magnitude of damage a single or multiple base lesions can cause in the iM structure. The present study can also help to search for potential iM forming regions in genomes, which were reported (56,58) to differ from the potentially G-quadruplex forming complementary regions. The conclusions following from the results may be also useful for designing new sensors and nano-devices.

SUPPLEMENTARY DATA

Supplementary Data are available at NAR online.

FUNDING

Czech Science Foundation [15-06785S, 17-12075S, 17-19170Y]; SYMBIT [CZ.02.1.01/0.0/0.0/15 003/0000477] financed by the ERDF. Funding for open access charge:

SYMBIT [CZ.02.1.01/0.0/0.0/15 003/0000477] financed by the ERDF.
Conflict of interest statement. None declared.

REFERENCES

1. Lindahl,T. (1993) Instability and decay of the primary structure of DNA. *Nature*, **362**, 709–715.
2. von Sonntag,C. (1987) New aspects in the free-radical chemistry of pyrimidine nucleobases. *Free Radic. Res. Commun.*, **2**, 217–224.
3. Konvalinova,H., Dvorakova,Z., Renciuk,D., Bednarova,K., Kejnovska,I., Trantirek,L., Vorlickova,M. and Sagi,J. (2015) Diverse effects of naturally occurring base lesions on the structure and stability of the human telomere DNA quadruplex. *Biochimie*, **118**, 15–25.
4. Sagi,J. (2014) G-quadruplexes incorporating modified constituents: a review. *J. Biomol. Struct. Dyn.*, **32**, 477–511.
5. Sagi,J. (2016) Designing G-quadruplex topologies by focusing on sequence modifications. In: *G-Quadruplex Structures, Formation and Role in Biology*. Nova Science Publishers, Inc., NY.
6. Gehring,K., Leroy,J.L. and Gueron,M. (1993) A tetrameric DNA structure with protonated cytosine.cytosine base pairs. *Nature*, **363**, 561–565.
7. Gueron,M. and Leroy,J.L. (2000) The i-motif in nucleic acids. *Curr. Opin. Struct. Biol.*, **10**, 326–331.
8. Day,H.A., Pavlou,P. and Waller,Z.A. (2014) i-Motif DNA: structure, stability and targeting with ligands. *Bioorg. Med. Chem.*, **22**, 4407–4418.
9. Brazier,J.A., Shah,A. and Brown,G.D. (2012) i-Motif formation in gene promoters: unusually stable formation in sequences complementary to known G-quadruplexes. *Chem. Commun. (Camb.)*, **48**, 10739–10741.
10. Sun,D. and Hurley,L.H. (2009) The importance of negative superhelicity in inducing the formation of G-quadruplex and i-motif structures in the c-Myc promoter: Implications for drug targeting and control of gene expression. *J. Med. Chem.*, **52**, 2863–2874.
11. Simonsson,T., Pribylova,M. and Vorlickova,M. (2000) A nuclease hypersensitive element in the human c-myc promoter adopts several distinct i-tetraplex structures. *Biochem. Biophys. Res. Commun.*, **278**, 158–166.
12. Skolakova,P., Foldynova-Trantirkova,S., Bednarova,K., Fiala,R., Vorlickova,M. and Trantirek,L. (2015) Unique C. elegans telomeric overhang structures reveal the evolutionarily conserved properties of telomeric DNA. *Nucleic. Acids. Res.*, **43**, 4733–4745.
13. Bhavsar-Jog,Y.P., Van Dornshuld,E., Brooks,T.A., Tschumper,G.S. and Wadkins,R.M. (2014) Epigenetic modification, dehydration, and molecular crowding effects on the thermodynamics of i-motif structure formation from C-rich DNA. *Biochemistry*, **53**, 1586–1594.
14. Selvam,S., Mandal,S. and Mao,H. (2017) Quantification of chemical and mechanical effects on the formation of the G-quadruplex and i-motif in duplex DNA. *Biochemistry*, **56**, 4616–4625.
15. Cui,J., Waltman,P., Le,V.H. and Lewis,E.A. (2013) The effect of molecular crowding on the stability of human c-MYC promoter sequence i-motif at neutral pH. *Molecules*, **18**, 12751–12767.
16. Dong,Y.C., Yang,Z.Q. and Liu,D.S. (2014) DNA nanotechnology based on i-motif structures. *Acc. Chem. Res.*, **47**, 1853–1860.
17. Nesterova,I.V. and Nesterov,E.E. (2014) Rational design of highly responsive pH sensors based on DNA i-motif. *J. Am. Chem. Soc.*, **136**, 8843–8846.
18. Benabou,S., Avino,A., Eritja,R., Gonzalez,C. and Gargallo,R. (2014) Fundamental aspects of the nucleic acid i-motif structures. *RSC Adv.*, **4**, 26956–26980.
19. Yang,B. and Rodgers,M.T. (2015) Base-pairing energies of protonated nucleoside base pairs of dCyd and m(5)dCyd: implications for the stability of DNA i-motif conformations. *J. Am. Soc. Mass Spectrom.*, **26**, 1394–1403.
20. Xu,B., Devi,G. and Shao,F. (2015) Regulation of telomeric i-motif stability by 5-methylcytosine and 5-hydroxymethylcytosine modification. *Org. Biomol. Chem.*, **13**, 5646–5651.
21. Canalia,M. and Leroy,J.L. (2005) Structure, internal motions and association-dissociation kinetics of the i-motif dimer of d(5mCCTCACTCC). *Nucleic Acids Res.*, **33**, 5471–5481.
22. Han,X., Leroy,J.L. and Gueron,M. (1998) An intramolecular i-motif: the solution structure and base-pair opening kinetics of d(5mCCT3CCT3ACCT3CC). *J. Mol. Biol.*, **278**, 949–965.
23. Nonin,S., Phan,A.T. and Leroy,J.L. (1997) Solution structure and base pair opening kinetics of the i-motif dimer of d(5mCCTTTACC): a noncanonical structure with possible roles in chromosome stability. *Structure*, **5**, 1231–1246.
24. Phan,A.T. and Leroy,J.L. (2000) Intramolecular i-motif structures of telomeric DNA. *J. Biomol. Struct. Dyn.*, **17**, (Suppl. 1), 245–251.
25. Lannes,L., Halder,S., Krishnan,Y. and Schwalbe,H. (2015) Tuning the pH response of i-motif DNA oligonucleotides. *ChemBioChem*, **16**, 1647–1656.
26. Reilly,S.M., Morgan,R.K., Brooks,T.A. and Wadkins,R.M. (2015) Effect of interior loop length on the thermal stability and pK(a) of i-motif DNA. *Biochemistry*, **54**, 1364–1370.
27. Fujii,T. and Sugimoto,N. (2015) Loop nucleotides impact the stability of intrastrand i-motif structures at neutral pH. *Phys. Chem. Chem. Phys.*, **17**, 16719–16722.
28. Gurung,S.P., Schwarz,C., Hall,J.P., Cardin,C.J. and Brazier,J.A. (2015) The importance of loop length on the stability of i-motif structures. *Chem. Commun. (Camb.)*, **51**, 5630–5632.
29. Lieblein,A.L., Furtig,B. and Schwalbe,H. (2013) Optimizing the kinetics and thermodynamics of DNA i-motif folding. *ChemBioChem*, **14**, 1226–1230.
30. McKim,M., Buxton,A., Johnson,C., Metz,A. and Sheardy,R.D. (2016) Loop sequence context influences the formation and stability of the i-motif for DNA oligomers of sequence (CCCXXX)4, where X = A and/or T, under slightly acidic conditions. *J. Phys. Chem. B*, **120**, 7652–7661.
31. Benabou,S., Garavis,M., Lyonnais,S., Eritja,R., Gonzalez,C. and Gargallo,R. (2016) Understanding the effect of the nature of the nucleobase in the loops on the stability of the i-motif structure. *Phys. Chem. Chem. Phys.*, **18**, 7997–8004.
32. Lee,I.J. and Kim,B.H. (2012) Monitoring i-motif transitions through the exciplex emission of a fluorescent probe incorporating two (Py)A units. *Chem. Commun. (Camb.)*, **48**, 2074–2076.
33. Pasternak,A. and Wengel,J. (2011) Modulation of i-motif thermodynamic stability by the introduction of UNA (unlocked nucleic acid) monomers. *Bioorg. Med. Chem. Lett.*, **21**, 752–755.
34. Perlikova,P., Karlsen,K.K., Pedersen,E.B. and Wengel,J. (2014) Unlocked nucleic acids with a pyrene-modified uracil: synthesis, hybridization studies, fluorescent properties and i-motif stability. *ChemBioChem*, **15**, 146–156.
35. Vorlickova,M., Tomasko,M., Sagi,A.J., Bednarova,K. and Sagi,J. (2012) 8-Oxoguanine in a quadruplex of the human telomere DNA sequence. *FEBS J.*, **279**, 29–39.
36. Skolakova,P., Bednarova,K., Vorlickova,M. and Sagi,J. (2010) Quadruplexes of human telomere dG(3)(TTAG(3))(3) sequences containing guanine abasic sites. *Biochem. Biophys. Res. Commun.*, **399**, 203–208.
37. Pfaffeneder,T., Spada,F., Wagner,M., Brandmayr,C., Laube,S.K., Eisen,D., Truss,M., Steinbacher,J., Hackner,B., Kotljarova,O. *et al.* (2014) Tet oxidizes thymine to 5-hydroxymethyluracil in mouse embryonic stem cell DNA. *Nat. Chem. Biol.*, **10**, 574–581.
38. Bransteitter,R., Pham,P., Scharff,M.D. and Goodman,M.F. (2003) Activation-induced cytidine deaminase deaminates deoxycytidine on single-stranded DNA but requires the action of RNase. *Proc. Natl. Acad. Sci. U.S.A.*, **100**, 4102–4107.
39. Schutsky,E.K., Nabel,C.S., Davis,A.K.F., DeNizio,J.E. and Kohli,R.M. (2017) APOBEC3A efficiently deaminates methylated, but not TET-oxidized, cytosine bases in DNA. *Nucleic. Acids. Res.*, **45**, 7655–7665.
40. Gray,D.M., Hung,S.H. and Johnson,K.H. (1995) Absorption and circular dichroism spectroscopy of nucleic acid duplexes and triplexes. *Methods Enzymol.*, **246**, 19–34.
41. Mergny,J.L. and Lacroix,L. (2003) Analysis of thermal melting curves. *Oligonucleotides*, **13**, 515–537.
42. Manzini,G., Yathindra,N. and Xodo,L.E. (1994) Evidence for intramolecularly folded i-DNA structures in biologically relevant CCC-repeat sequences. *Nucleic. Acids. Res.*, **22**, 4634–4640.
43. Sagi,J. (2017) In what ways do synthetic nucleotides and natural base lesions alter the structural stability of G-quadruplex nucleic acids? *J. Nucleic. Acids*, **2017**, 1641845.

44. Aggrawal,M., Joo,H., Liu,W.B., Tsai,J. and Xue,L. (2012) 8-Oxo-7,8-dihydrodeoxyadenosine: The first example of a native DNA lesion that stabilizes human telomeric G-quadruplex DNA. *Biochem. Biophys. Res. Commun.*, **421**, 671–677.
45. Babinsky,M., Fiala,R., Kejnovska,I., Bednarova,K., Marek,R., Sagi,J., Sklenar,V. and Vorlickova,M. (2014) Loss of loop adenines alters human telomere d AG(3)(TTAG(3))(3) quadruplex folding. *Nucleic. Acids. Res.*, **42**, 14031–14041.
46. Virgilio,A., Esposito,V., Mayol,L., Giancola,C., Petraccone,L. and Galeone,A. (2015) The oxidative damage to the human telomere: effects of 5-hydroxymethyl-2'-deoxyuridine on telomeric G-quadruplex structures. *Org. Biomol. Chem.*, **13**, 7421–7429.
47. Kejnovska,I., Bednarova,K., Renciuk,D., Dvorakova,Z., Skolakova,P., Trantirek,L., Fiala,R., Vorlickova,M. and Sagi,J. (2017) Clustered abasic lesions profoundly change the structure and stability of human telomeric G-quadruplexes. *Nucleic Acids Res.*, **45**, 4294–4305.
48. Virgilio,A., Petraccone,L., Esposito,V., Citarella,G., Giancola,C. and Galeone,A. (2012) The abasic site lesions in the human telomeric sequence d[TA(G(3)T(2)A)(3)G(3)]: a thermodynamic point of view. *Biochim. Biophys. Acta*, **1820**, 2037–2043.
49. Phan,A.T., Gueron,M. and Leroy,J.L. (2000) The solution structure and internal motions of a fragment of the cytidine-rich strand of the human telomere. *J. Mol. Biol.*, **299**, 123–144.
50. Esmaili,N. and Leroy,J.L. (2005) i-Motif solution structure and dynamics of the d(AACCCC) and d(CCCCAA) tetrahymena telomeric repeats. *Nucleic. Acids. Res.*, **33**, 213–224.
51. Lieblein,A.L., Buck,J., Schlepckow,K., Fürtig,B. and Schwalbe,H. (2012) Time-resolved NMR spectroscopic studies of DNA i-motif folding reveal kinetic partitioning. *Angew. Chem. Int. Ed. Engl.*, **51**, 250–253.
52. Tomasko,M., Vorlickova,M. and Sagi,J. (2009) Substitution of adenine for guanine in the quadruplex-forming human telomere DNA sequence G(3)(T(2)AG(3))(3). *Biochimie*, **91**, 171–179.
53. Kang,H.J., Kendrick,S., Hecht,S.M. and Hurley,L.H. (2014) The transcriptional complex between the BCL2 i-motif and hnRNP LL is a molecular switch for control of gene expression that can be modulated by small molecules. *J. Am. Chem. Soc.*, **136**, 4172–4185.
54. Brown,R.V., Wang,T., Chappeta,V.R., Wu,G., Onel,B., Chawla,R., Quijada,H., Camp,S.M., Chiang,E.T., Lassiter,Q.R. *et al.* (2017) The consequences of overlapping G-quadruplexes and i-motifs in the platelet-derived growth factor receptor beta core promoter nuclease hypersensitive element can explain the unexpected effects of mutations and provide opportunities for selective targeting of both structures by small molecules to downregulate gene expression. *J. Am. Chem. Soc.*, **139**, 7456–7475.
55. Renciuk,D., Rynes,J., Kejnovska,I., Foldynova-Trantirkova,S., Andang,M., Trantirek,L. and Vorlickova,M. (2017) G-quadruplex formation in the Oct4 promoter positively regulates Oct4 expression. *Biochim. Biophys. Acta*, **1860**, 175–183.
56. Wright,E.P., Huppert,J.L. and Waller,Z.A.E. (2017) Identification of multiple genomic DNA sequences which form i-motif structures at neutral pH. *Nucleic Acids Res.*, **45**, 2951–2959.
57. Kaiser,C.E., Van Ert,N.A., Agrawal,P., Chawla,R., Yang,D. and Hurley,L.H. (2017) Insight into the complexity of the i-motif and G-quadruplex DNA structures formed in the KRAS promoter and subsequent drug-induced gene repression. *J. Am. Chem. Soc.*, **139**, 8522–8536.
58. Dhakal,S., Yu,Z.B., Konik,R., Cui,Y.X., Koirala,D. and Mao,H.B. (2012) G-quadruplex and i-motif are mutually exclusive in ILPR double-stranded DNA. *Biophys. J.*, **102**, 2575–2584.